Transverse Energy Distributions within Jets in $p\bar{p}$ Collisions at $\sqrt{s} = 1.8$ TeV

The DØ Collaboration[1]

(July 1995)

The distribution of the transverse energy in jets has been measured in $p\bar{p}$ collisions at $\sqrt{s} = 1.8$ TeV using the DØ detector at Fermilab. This measurement of the jet shape is made as a function of jet transverse energy in both the central and forward rapidity regions. Jets are observed to narrow both with increasing transverse energy and with increasing rapidity. Next-to-leading order partonic QCD calculations are compared to the data. Although the calculations qualitatively describe the data, they are shown to be very dependent on renormalization scale, parton clustering algorithm and jet direction definition and fail to consistently describe the data in all regions.

S. Abachi,[12] B. Abbott,[34] M. Abolins,[23] B.S. Acharya,[41] I. Adam,[10] D.L. Adams,[35] M. Adams,[15] S. Ahn,[12] H. Aihara,[20] J. Alitti,[37] G. Álvarez,[16] G.A. Alves,[8] E. Amidi,[27] N. Amos,[22] E.W. Anderson,[17] S.H. Aronson,[3] R. Astur,[39] R.E. Avery,[29] A. Baden,[21] V. Balamurali,[30] J. Balderston,[14] B. Baldin,[12] J. Bantly,[4] J.F. Bartlett,[12] K. Bazizi,[7] J. Bendich,[20] S.B. Beri,[32] I. Bertram,[35] V.A. Bezzubov,[33] P.C. Bhat,[12] V. Bhatnagar,[32] M. Bhattacharjee,[11] A. Bischoff,[7] N. Biswas,[30] G. Blazey,[12] S. Blessing,[13] P. Bloom,[5] A. Boehnlein,[12] N.I. Bojko,[33] F. Borcherding,[12] J. Borders,[36] C. Boswell,[7] A. Brandt,[12] R. Brock,[23] A. Bross,[12] D. Buchholz,[29] V.S. Burtovoi,[33] J.M. Butler,[12] D. Casey,[36] H. Castilla-Valdez,[9] D. Chakraborty,[39] S.-M. Chang,[27] S.V. Chekulaev,[33] L.-P. Chen,[20] W. Chen,[39] L. Chevalier,[37] S. Chopra,[32] B.C. Choudhary,[7] J.H. Christenson,[12] M. Chung,[15] D. Claes,[39] A.R. Clark,[20] W.G. Cobau,[21] J. Cochran,[7] W.E. Cooper,[12] C. Cretsinger,[36] D. Cullen-Vidal,[4] M.A.C. Cummings,[14] D. Cutts,[4] O.I. Dahl,[20] K. De,[42] M. Demarteau,[12] R. Demina,[27] K. Denisenko,[12] N. Denisenko,[12] D. Denisov,[12] S.P. Denisov,[33] W. Dharmaratna,[13] H.T. Diehl,[12] M. Diesburg,[12] G. Di Loreto,[23] R. Dixon,[12] P. Draper,[42] J. Drinkard,[6] Y. Ducros,[37] S.R. Dugad,[41] S. Durston-Johnson,[36] D. Edmunds,[23] J. Ellison,[7] V.D. Elvira,[12,‡] R. Engelmann,[39] S. Eno,[21] G. Eppley,[35] P. Ermolov,[24] O.V. Eroshin,[33] V.N. Evdokimov,[33] S. Fahey,[23] T. Fahland,[4] M. Fatyga,[3] M.K. Fatyga,[36] J. Featherly,[3] S. Feher,[39] D. Fein,[2] T. Ferbel,[36] G. Finocchiaro,[39] H.E. Fisk,[12] Yu. Fisyak,[24] E. Flattum,[23] G.E. Forden,[2] M. Fortner,[28] K.C. Frame,[23] P. Franzini,[10] S. Fuess,[12] A.N. Galjaev,[33] E. Gallas,[42] C.S. Gao,[12,*] S. Gao,[12,*] T.L. Geld,[23] R.J. Genik II,[23] K. Genser,[12] C.E. Gerber,[12,§] B. Gibbard,[3] V. Glebov,[36] S. Glenn,[5] B. Gobbi,[29] M. Goforth,[13] A. Goldschmidt,[20] B. Gómez,[1] P.I. Goncharov,[33] H. Gordon,[3] L.T. Goss,[43] N. Graf,[3] P.D. Grannis,[39] D.R. Green,[12] J. Green,[28] H. Greenlee,[12] G. Griffin,[6] N. Grossman,[12] P. Grudberg,[20] S. Grünendahl,[36] W. Gu,[12,*] G. Guglielmo,[31] J.A. Guida,[39] J.M. Guida,[3] W. Guryn,[3] S.N. Gurzhiev,[33] P. Gutierrez,[31] Y.E. Gutnikov,[33] N.J. Hadley,[21] H. Haggerty,[12] S. Hagopian,[13] V. Hagopian,[13] K.S. Hahn,[36] R.E. Hall,[6] S. Hansen,[12] R. Hatcher,[23] J.M. Hauptman,[17] D. Hedin,[28] A.P. Heinson,[7] U. Heintz,[12] R. Hernández-Montoya,[9] T. Heuring,[13] R. Hirosky,[13] J.D. Hobbs,[12] B. Hoeneisen,[1,¶] J.S. Hoftun,[4] F. Hsieh,[22] Ting Hu,[39] Tong Hu,[16] T. Huehn,[7] S. Igarashi,[12] A.S. Ito,[12] E. James,[2] J. Jaques,[30] S.A. Jerger,[23] J.Z.-Y. Jiang,[39] T. Joffe-Minor,[29] H. Johari,[27] K. Johns,[2] M. Johnson,[12] H. Johnstad,[40]

[1]Submitted to the International Europhysics Conference on High Energy Physics (HEP 95), Brussels, Belgium, 27 July - 2 August 1995.

A. Jonckheere,[12] M. Jones,[14] H. Jöstlein,[12] S.Y. Jun,[29] C.K. Jung,[39] S. Kahn,[3] G. Kalbfleisch,[31] J.S. Kang,[18] R. Kehoe,[30] M.L. Kelly,[30] A. Kernan,[7] L. Kerth,[20] C.L. Kim,[18] S.K. Kim,[38] A. Klatchko,[13] B. Klima,[12] B.I. Klochkov,[33] C. Klopfenstein,[39] V.I. Klyukhin,[33] V.I. Kochetkov,[33] J.M. Kohli,[32] D. Koltick,[34] A.V. Kostritskiy,[33] J. Kotcher,[3] J. Kourlas,[26] A.V. Kozelov,[33] E.A. Kozlovski,[33] M.R. Krishnaswamy,[41] S. Krzywdzinski,[12] S. Kunori,[21] S. Lami,[39] G. Landsberg,[12] R.E. Lanou,[4] J-F. Lebrat,[37] A. Leflat,[24] H. Li,[39] J. Li,[42] Y.K. Li,[29] Q.Z. Li-Demarteau,[12] J.G.R. Lima,[8] D. Lincoln,[22] S.L. Linn,[13] J. Linnemann,[23] R. Lipton,[12] Y.C. Liu,[29] F. Lobkowicz,[36] S.C. Loken,[20] S. Lökös,[39] L. Lueking,[12] A.L. Lyon,[21] A.K.A. Maciel,[8] R.J. Madaras,[20] R. Madden,[13] I.V. Mandrichenko,[33] Ph. Mangeot,[37] S. Mani,[5] B. Mansoulié,[37] H.S. Mao,[12,*] S. Margulies,[15] R. Markeloff,[28] L. Markosky,[2] T. Marshall,[16] M.I. Martin,[12] M. Marx,[39] B. May,[29] A.A. Mayorov,[33] R. McCarthy,[39] T. McKibben,[15] J. McKinley,[23] T. McMahon,[31] H.L. Melanson,[12] J.R.T. de Mello Neto,[8] K.W. Merritt,[12] H. Miettinen,[35] A. Milder,[2] A. Mincer,[26] J.M. de Miranda,[8] C.S. Mishra,[12] M. Mohammadi-Baarmand,[39] N. Mokhov,[12] N.K. Mondal,[41] H.E. Montgomery,[12] P. Mooney,[1] M. Mudan,[26] C. Murphy,[16] C.T. Murphy,[12] F. Nang,[4] M. Narain,[12] V.S. Narasimham,[41] A. Narayanan,[2] H.A. Neal,[22] J.P. Negret,[1] E. Neis,[22] P. Nemethy,[26] D. Nešić,[4] D. Norman,[43] L. Oesch,[22] V. Oguri,[8] E. Oltman,[20] N. Oshima,[12] D. Owen,[23] P. Padley,[35] M. Pang,[17] A. Para,[12] C.H. Park,[12] Y.M. Park,[19] R. Partridge,[4] N. Parua,[41] M. Paterno,[36] J. Perkins,[42] A. Peryshkin,[12] M. Peters,[14] H. Piekarz,[13] Y. Pischalnikov,[34] A. Pluquet,[37] V.M. Podstavkov,[33] B.G. Pope,[23] H.B. Prosper,[13] S. Protopopescu,[3] D. Pušeljić,[20] J. Qian,[22] P.Z. Quintas,[12] R. Raja,[12] S. Rajagopalan,[39] O. Ramirez,[15] M.V.S. Rao,[41] P.A. Rapidis,[12] L. Rasmussen,[39] A.L. Read,[12] S. Reucroft,[27] M. Rijssenbeek,[39] T. Rockwell,[23] N.A. Roe,[20] P. Rubinov,[39] R. Ruchti,[30] S. Rusin,[24] J. Rutherfoord,[2] A. Santoro,[8] L. Sawyer,[42] R.D. Schamberger,[39] H. Schellman,[29] J. Sculli,[26] E. Shabalina,[24] C. Shaffer,[13] H.C. Shankar,[41] R.K. Shivpuri,[11] M. Shupe,[2] J.B. Singh,[32] V. Sirotenko,[28] W. Smart,[12] A. Smith,[2] R.P. Smith,[12] R. Snihur,[29] G.R. Snow,[25] S. Snyder,[39] J. Solomon,[15] P.M. Sood,[32] M. Sosebee,[42] M. Souza,[8] A.L. Spadafora,[20] R.W. Stephens,[42] M.L. Stevenson,[20] D. Stewart,[22] D.A. Stoianova,[33] D. Stoker,[6] K. Streets,[26] M. Strovink,[20] A. Taketani,[12] P. Tamburello,[21] J. Tarazi,[6] M. Tartaglia,[12] T.L. Taylor,[29] J. Teiger,[37] J. Thompson,[21] T.G. Trippe,[20] P.M. Tuts,[10] N. Varelas,[23] E.W. Varnes,[20] P.R.G. Virador,[20] D. Vititoe,[2] A.A. Volkov,[33] A.P. Vorobiev,[33] H.D. Wahl,[13] G. Wang,[13] J. Wang,[12,*] L.Z. Wang,[12,*] J. Warchol,[30] M. Wayne,[30] H. Weerts,[23] F. Wen,[13] W.A. Wenzel,[20] A. White,[42] J.T. White,[43] J.A. Wightman,[17] J. Wilcox,[27] S. Willis,[28] S.J. Wimpenny,[7] J.V.D. Wirjawan,[43] J. Womersley,[12] E. Won,[36] D.R. Wood,[12] H. Xu,[4] R. Yamada,[12] P. Yamin,[3] C. Yanagisawa,[39] J. Yang,[26] T. Yasuda,[27] C. Yoshikawa,[14] S. Youssef,[13] J. Yu,[36] Y. Yu,[38] Y. Zhang,[12,*] Y.H. Zhou,[12,*] Q. Zhu,[26] Y.S. Zhu,[12,*] Z.H. Zhu,[36] D. Zieminska,[16] A. Zieminski,[16] and A. Zylberstejn[37]

[1] Universidad de los Andes, Bogotá, Colombia
[2] University of Arizona, Tucson, Arizona 85721
[3] Brookhaven National Laboratory, Upton, New York 11973
[4] Brown University, Providence, Rhode Island 02912
[5] University of California, Davis, California 95616
[6] University of California, Irvine, California 92717
[7] University of California, Riverside, California 92521
[8] LAFEX, Centro Brasileiro de Pesquisas Físicas, Rio de Janeiro, Brazil
[9] CINVESTAV, Mexico City, Mexico
[10] Columbia University, New York, New York 10027
[11] Delhi University, Delhi, India 110007
[12] Fermi National Accelerator Laboratory, Batavia, Illinois 60510
[13] Florida State University, Tallahassee, Florida 32306
[14] University of Hawaii, Honolulu, Hawaii 96822

[15]University of Illinois at Chicago, Chicago, Illinois 60607
[16]Indiana University, Bloomington, Indiana 47405
[17]Iowa State University, Ames, Iowa 50011
[18]Korea University, Seoul, Korea
[19]Kyungsung University, Pusan, Korea
[20]Lawrence Berkeley Laboratory and University of California, Berkeley, California 94720
[21]University of Maryland, College Park, Maryland 20742
[22]University of Michigan, Ann Arbor, Michigan 48109
[23]Michigan State University, East Lansing, Michigan 48824
[24]Moscow State University, Moscow, Russia
[25]University of Nebraska, Lincoln, Nebraska 68588
[26]New York University, New York, New York 10003
[27]Northeastern University, Boston, Massachusetts 02115
[28]Northern Illinois University, DeKalb, Illinois 60115
[29]Northwestern University, Evanston, Illinois 60208
[30]University of Notre Dame, Notre Dame, Indiana 46556
[31]University of Oklahoma, Norman, Oklahoma 73019
[32]University of Panjab, Chandigarh 16-00-14, India
[33]Institute for High Energy Physics, 142-284 Protvino, Russia
[34]Purdue University, West Lafayette, Indiana 47907
[35]Rice University, Houston, Texas 77251
[36]University of Rochester, Rochester, New York 14627
[37]CEA, DAPNIA/Service de Physique des Particules, CE-SACLAY, France
[38]Seoul National University, Seoul, Korea
[39]State University of New York, Stony Brook, New York 11794
[40]SSC Laboratory, Dallas, Texas 75237
[41]Tata Institute of Fundamental Research, Colaba, Bombay 400005, India
[42]University of Texas, Arlington, Texas 76019
[43]Texas A&M University, College Station, Texas 77843

INTRODUCTION

Next-to-leading order (NLO) QCD calculations describe many experimental results well (1), including inclusive jet and di-jet production. These NLO predictions, which are at the parton level and ignore fragmentation, are the first order that allow a meaningful description of the internal structure of jets, created by parton radiation. We test whether these predictions can accurately describe the observed shape of jets, by comparing the transverse energy distributions within jets.

This paper describes a measurement of the shape of jets as a function of jet transverse energy and rapidity using the DØ detector (2). Other experiments have measured the shape of centrally produced jets using only charged particles (3) and using charged and neutral particles (4). In this analysis, both neutral and charged particles contribute to the measurement of the jet shape which is extended to the previously unexplored forward rapidity region.

DATA ANALYSIS

This measurement was performed using the DØ calorimeters which provide large angular coverage and fine segmentation (0.1×0.1 in $\Delta\eta \times \Delta\phi$, where $\eta \equiv -\ln[\tan(\theta/2)]$ is the pseudorapidity, and θ and ϕ are the polar and azimuthal angles). We use a right handed

coordinate system with the positive z-axis along the proton direction and the y-axis defined as the vertical. The calorimeters provide hermetic and uniform coverage for $|\eta| < 4.0$. The energy E resolution for electromagnetic showers is $\approx 15\%/\sqrt{E}$ and the single particle hadronic energy resolution is $\approx 50\%/\sqrt{E}$.

The data used in this analysis (5) were taken during the 1992-1993 run of the Tevatron. Four separate hardware triggers were used, each requiring the transverse energy E_T in a specified number of trigger towers ($\Delta\eta \times \Delta\phi$ =0.2 $\times$ 0.2) to exceed various thresholds. The selected events were also subjected to a software trigger which required a reconstructed jet, using a fixed cone algorithm with radius $\mathcal{R} = \sqrt{(\Delta\eta)^2 + (\Delta\phi)^2}$ equal to 0.7, above a set E_T threshold. To remove trigger biases, the E_T of the leading jet in each event was required to be in a region of full trigger efficiency. These events were used to populate four non-overlapping jet E_T ranges of 45-70, 70-105, 105-140 and greater than 140 GeV.

In the offline reconstruction, the event vertex was required to be within $\pm$ 30 cm of the detector center to keep the geometry projective. All jets that passed quality requirements to remove spurious jets were considered (6). Jets were analyzed in a central region of $|\eta| \leq 0.2$ and a forward region of $2.5 \leq |\eta| \leq 3.0$.

For this analysis, jets were reconstructed using a fixed cone algorithm with $\mathcal{R} = 1.0$. Calorimeter towers (0.1×0.1 in $\Delta\eta \times \Delta\phi$) with energy greater than 1.0 GeV were used as seeds for finding preclusters, which were formed by adding neighboring towers within a radius of 0.3. A cone of radius 1.0 was drawn around each precluster and a new jet center was calculated using the Snowmass (7) jet direction definitions: $\eta_{jet} = \sum_i E_{Ti}\eta_i / \sum_i E_{Ti}$; $\phi_{jet} = \sum_i E_{Ti}\phi_i / \sum_i E_{Ti}$. The sums extend over all towers, i, within the cone. This process was repeated until a stable jet center was found. Then the jet direction was redefined using the DØ jet direction definitions: $\eta_{jet} = -\ln(\tan(\theta_{jet}/2))$; $\phi_{jet} = \tan^{-1}(\sum_i E_{yi} / \sum_i E_{xi})$ where $\theta_{jet} = \tan^{-1}\sqrt{(\sum_i E_{xi})^2 + (\sum_i E_{yi})^2} / \sum_i E_{zi}$ and the transverse energy of the jet was defined as $E_T = \sum_i E_i \sin(\theta_i)$. After a preliminary set of jets was found, overlapping jets were redefined. Two jets were merged into one jet if more than 50% of the E_T of the jet with the smaller E_T was contained in the overlap region. The direction of the new jet was defined as the vector sum of the two original jet momenta, and the energy was recalculated. If less than 50% of the E_T was contained in the overlap region, the jets were split into two distinct jets. In this case, the energy of each calorimeter cell in the overlap region was assigned to the nearest jet and the jet directions were recalculated.

A scale correction (6) was applied to all jets to correct for the calorimeter energy response and for effects of the hardware suppression of the asymmetric pedestal distribution. Energy in the jet due to the underlying event from spectator interactions was also removed. This energy scale correction was a function of η and E_T and increased the jet energy by approximately 15-25%. The corrected jet E_T was used only to determine which data set a jet populated. Energy leaking out of the $\mathcal{R} = 1.0$ jet cone due to showering in the calorimeter was measured to be less than 2% in all regions.

The jet cone was divided into 10 subcones centered on the jet axis with radii r varying from 0.1 to 1.0 in $\Delta r = 0.1$ increments. The jet shape, $\rho(r)$, is defined as the average fraction of calorimeter cell E_T in a subcone of radius r: $\rho(r) = \frac{1}{N_{jets}} \sum_{jets} \frac{E_T(r)}{E_T(r=1)}$, where N_{jets} is the number of jets in the sample. A calorimeter cell was considered to be within a subcone if the center of the cell was located within the subcone boundary. (The scale correction described above was not applied to the subcone E_T.) By definition, $\rho(1) = 1$. At a given value of r, $\rho(r)$ is larger for narrower jets than for broader jets.

The subcone E_T was corrected to remove energy in the jet due to the underlying event and due to the hardware pedestal suppression. A sample of minimum bias events was analyzed to determine the E_T within each calorimeter tower due to these effects. An η-independent

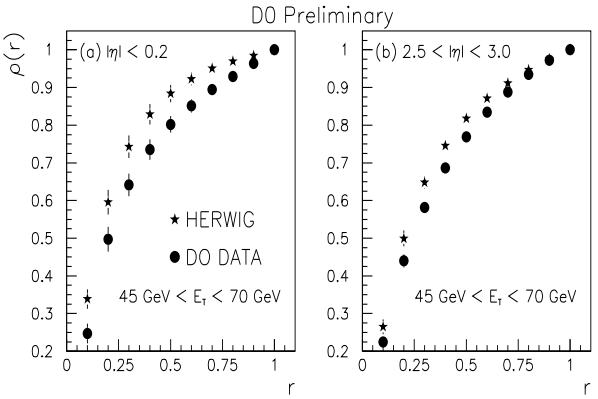

FIG. 1. The average integrated E_T fraction versus the radial distance from the jet axis is plotted for DØ data and HERWIG Monte Carlo, before effects due to the calorimetric measurement are removed, for the E_T range 45-70 GeV for (a) $|\eta| \leq 0.2$ and (b) $2.5 \leq |\eta| \leq 3.0$.

correction of approximately 6 MeV (12 MeV for events with multiple interactions) was applied to each calorimeter tower in the subcone to remove E_T due to the underlying event. The energy due to the hardware pedestal suppression was removed from the subcones using an η-dependent correction applied to each calorimeter tower which varied from an E_T of 14 MeV to 7 MeV in the central region, and from 6 MeV to 1 MeV in the forward region.

In Fig. 1, the average integrated E_T fraction versus the radial distance from the jet axis is shown in the two η regions for jets with E_T between 45 and 70 GeV. Also shown are results from the HERWIG (8) parton shower Monte Carlo which includes fragmentation effects and a full DØ detector simulation using GEANT (9). Both the data and HERWIG include effects due to the calorimetric measurement, which will be discussed below. In both the central and forward regions, the measured jets are broader than predicted by the Monte Carlo simulations.

In order to compare different data samples and the data to theoretical predictions, the effects of the calorimetric measurement on the jet shape must be removed. The calorimeter can influence the jet shape by artificially narrowing the jet because of a decrease in response to low energy particles which predominate at large radii and by widening the jet due to shower spreading. As the energy of the jet increases, the non-linear response at low energy is less important. Showering effects are more pronounced in the forward regions because of the smaller geometrical size of towers, which are of equal size in all regions in $\eta - \phi$ space.

Monte Carlo simulations were used to examine the jet shape before and after detector modelling and to provide correction factors which remove the effects of the calorimetric measurement, allowing the jet shapes to be measured at the particle level. These effects depend upon the fragmentation and therefore three simulations with different fragmentation schemes (HERWIG, ISAJET (10), PYTHIA (11)), using full GEANT calorimeter and hadron shower modelling, were used to determine correction factors. Each simulation produced different jet shapes, however, the difference between the shape before and after detector modelling was within 3% for all the simulations. In the inner subcone, where the correction is largest, the jets were corrected by $\approx$ 9% in the central region and $\approx$ 28% in the forward region.

Systematic uncertainties were determined for each value of $\rho(r)$ in all regions of jet η and E_T. The uncertainties in the energy deposited by spectator interactions and the hardware

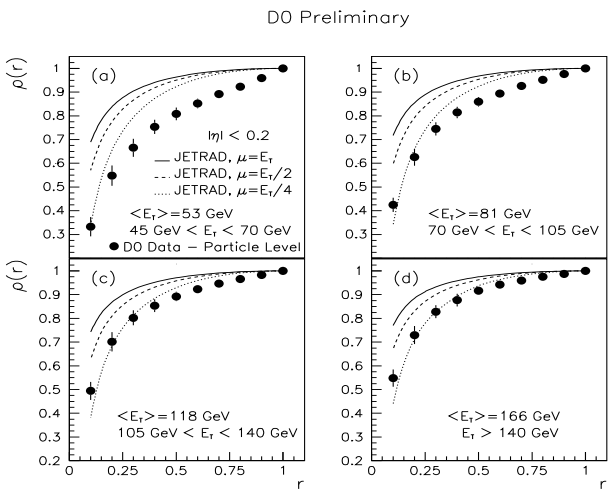

FIG. 2. The measured jet shapes, with effects due to the calorimetric measurement removed, compared to NLO predictions with three renormalization scales for $|\eta| \leq 0.2$ for the jet E_T range (a) 45-70 GeV, (b) 70-105 GeV, (c) 105-140 GeV, (d) greater than 140 GeV.

pedestal suppression were determined by varying the corrections by their measured errors. Each contributed an error of less than 0.5% to any value of $\rho(r)$. The jet scale correction was varied within its measured uncertainty and caused an error of less than 1% on the jet shape, which arises from jets migrating to different energy ranges. Monte Carlo studies show that lower energy particles predominate at large radii. This causes an uncertainty due to the uniform application of the calorimeter energy response correction in the jet scale correction. To determine the error due to the energy response, various low energy calorimeter response curves were simulated in the Monte Carlo, yielding a difference of $\approx$ 3% in the measured jet shape, which was assigned as a systematic error. A Monte Carlo calculation of the jet shapes was performed with and without the jet quality requirements. These requirements were found to cause an uncertainty of less than 1% in any data point. The uncertainty in the jet shape due to the correction to the particle level was assigned as the 3% difference between the correction factors obtained from the three simulations. The above systematic errors were added in quadrature with the statistical error to obtain the final errors on the jet shape which varied from 3 to 4% for $r < 0.5$ and were $< 2\%$ for $r > 0.5$.

RESULTS AND COMPARISON TO NLO PREDICTIONS

The jet shapes at the particle level (calorimetric measurement effects removed) are shown for centrally produced jets in Fig. 2 for four E_T ranges. Jets are observed to narrow as the jet E_T increases. This is in qualitative agreement with the measurement using charged particle distributions by CDF (3) at a comparable jet E_T.

The data in Fig. 2 are compared to the jet shapes calculated using JETRAD (12), an exact NLO tree and loop partonic QCD prediction. At this order, $\mathcal{O}(\alpha_s^3)$, there can be two or three partons in the final state. Substructure occurs in jets when two final state partons are clustered together into a single jet. To approximate the experimental jet algorithm, two partons are clustered into one jet, using the η and ϕ values previously defined, if they are within a distance of 1.0 of each other in $\eta - \phi$ space. The energies of these jets are defined

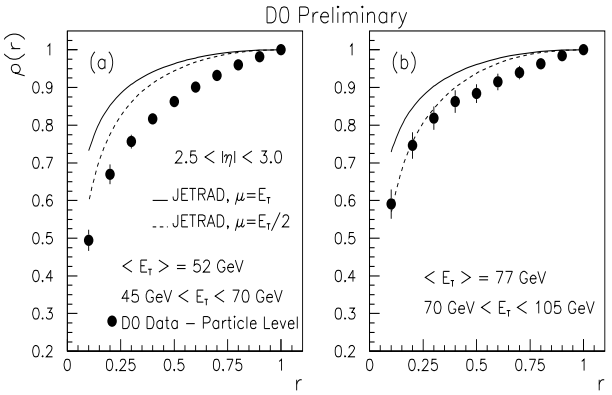

FIG. 3. The measured jet shapes, with effects due to the calorimetric measurement removed, compared to NLO predictions with two renormalization scales for $2.5 \leq |\eta| \leq 3.0$ for the jet E_T range (a) 45-70 GeV and (b) 70-105 GeV.

as the sum of the energies of the partons in the jets and the jet directions are the vector sums of the momenta of the partons. The jet shape predictions were calculated in the same E_T and η ranges as the data, using the CTEQ2M (13) parton distribution function (pdf) and three values of the renormalization scale, $\mu = E_T$, $E_T/2$, and $E_T/4$. They were also calculated using the MRSD− (14) pdf and were found to be insensitive to this change. At the lower two jet E_T ranges, the theory is narrower than the data for all values of μ and is narrower for all values except $\mu = E_T/4$ for the higher two E_T ranges. Both the data and the theoretical predictions narrow with increasing jet E_T but the measured jets narrow more quickly than the predictions.

Figure 3 shows the measured jet shapes, in the forward region for two jet E_T ranges. The measured jets are observed to narrow with increasing jet E_T. Comparing Figs. 2 and 3, it is observed that jets of the same E_T are narrower in the forward region than in the central region. Comparisons to the JETRAD predictions in the forward region are shown using two values of the renormalization scale. The theoretically predicted jet shapes are narrower than the data in both E_T ranges and do not narrow with increasing jet E_T. As observed in the data, the theoretically predicted jet shapes are narrower in the forward region than in the central for jets of the same E_T, but they do not narrow as quickly as the data.

Comparison of HERWIG simulations of jet shapes before fragmentation (parton level) and after (particle level) shows that the effects of fragmentation processes are important and tend to broaden the jets in both the central and forward regions.

Although the experimental cone algorithm is well defined, it is impossible to simulate exactly in the theoretical prediction. We have investigated the effect on the jet shape when using different parton clustering algorithms in the predictions as shown in Fig. 4. The JETRAD clustering algorithm was described previously. The JETRAD-2 algorithm clusters two partons into a single jet if they are each within a distance of 1.0 of their vector sum, creating jets with the same radius as in the experimental measurement. An alternate theoretical prediction uses the R_{Sep}=1.3 algorithm (15) with the HMRSB (16) pdf. This algorithm clusters two partons into a single jet if they are each within a distance of 1.0 of their vector sum and if they are within a distance of 1.3 of each other. This extra constraint is expected to better simulate the experimentally measured jets (15). The predictions vary widely depending upon the choice of parton clustering algorithm and no one algorithm

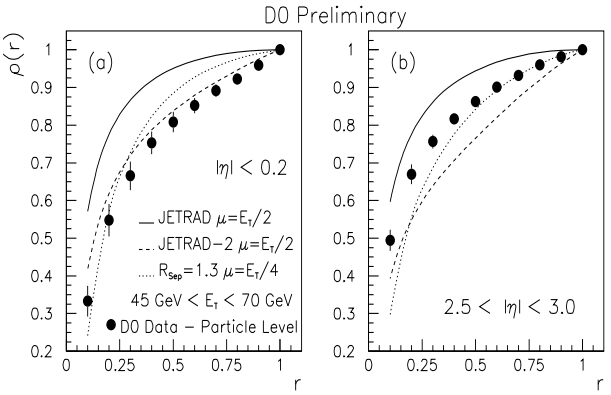

FIG. 4. The measured jet shapes at the particle level for jets with $45 < E_T < 70$ compared to NLO predictions for different parton clustering algorithms for (a) $|\eta| \leq 0.2$ and (b) $2.5 \leq |\eta| \leq 3.0$.

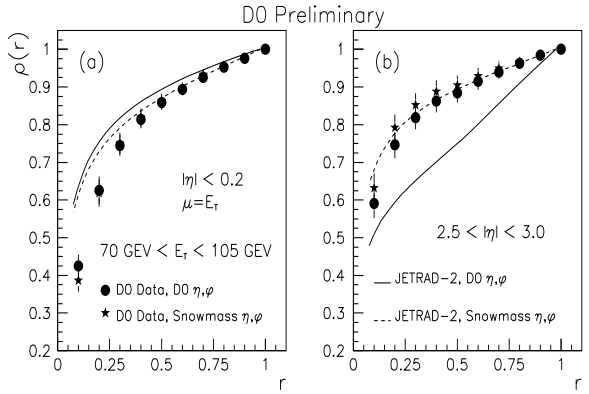

FIG. 5. Comparisons of jet shapes from data and NLO predictions using different jet direction definitions for jets with $70 < E_T < 105$ and for (a) $|\eta| \leq 0.2$ and (b) $2.5 \leq |\eta| \leq 3.0$.

consistently describes the data in both the central and forward regions.

The definition of the jet direction influences both the data and theoretical predictions. The effects on the jet shape when changing the final jet direction from the DØ definition to the Snowmass definition were investigated. Figure 5 shows the measured jet shapes and using the two η and ϕ definitions and comparisons to the predictions using the JETRAD-2 parton clustering algorithm. In the central region, the jet shape measured using the DØ definition is narrower than when using the Snowmass definition by $\sim 3\%$ in the inner subcone. In the forward region the Snowmass definition produces jets which are narrower by $\sim 5\%$ in the inner subcone. The theoretical predictions exhibit the same behavior, but the differences between the shapes using the two definitions are larger. The measured jets are narrower in the forward region than in the central for jets of the same E_T using either η and ϕ definition. The predicted shapes are narrower in the forward than the central region using the Snowmass definition but display the opposite behavior using the DØ definition. In summary, it is observed that the experimental data are relatively insensitive to the choice of jet direction definition, whereas the theoretical predictions are very sensitive.

CONCLUSIONS

Partonic theory of jet production at leading order, in which each jet is described by a single parton, cannot make a meaningful prediction of the jet shape. Because the jet shape measurement is a first order prediction at partonic NLO, large effects due to the uncertainty in the renormalization scale are expected and seen. NLO calculations can qualitatively describe the jet shape, but are very sensitive to both the parton clustering algorithm and the jet direction definition. The predictions do not consistently describe the jet shapes in all regions with a particular choice of parameters.

In summary, we have measured the jet shapes as a function of E_T and η. In the central and forward regions, jets become narrower with increasing jet E_T. Jets at the same E_T are narrower in the forward region than in the central region. The NLO partonic calculations do not presently reproduce the detailed behavior of the data.

ACKNOWLEDGEMENTS

We thank Walter Giele for many helpful discussions concerning the use of JETRAD and Stephen Ellis for his theoretical predictions. We thank the Fermilab Accelerator, Computing, and Research Divisions, and the support staffs at the collaborating institutions for their contributions to the success of this work. We also acknowledge the support of the U.S. Department of Energy, the U.S. National Science Foundation, the Commissariat à L'Energie Atomique in France, the Ministry for Atomic Energy and the Ministry of Science and Technology Policy in Russia, CNPq in Brazil, the Departments of Atomic Energy and Science and Education in India, Colciencias in Colombia, CONACyT in Mexico, the Ministry of Education, Research Foundation and KOSEF in Korea and the A.P. Sloan Foundation.

REFERENCES

* Visitor from IHEP, Beijing, China.
‡ Visitor from CONICET, Argentina.
§ Visitor from Universidad de Buenos Aires, Argentina.
¶ Visitor from Univ. San Francisco de Quito, Ecuador.

1. W.T. Giele, E.W.N. Glover and D.A. Kosower, Phys. Rev. Lett. **73**, 2019 (1994); S.D. Ellis, Z. Kunszt, and D.E. Soper, Phys. Rev. Lett. **69** 1496 (1992); S.D. Ellis, Z. Kunszt, and D.E. Soper, Phys. Rev. Lett. **64** 2121 (1990);
2. DØ collaboration, S. Abachi *et al.*, Nucl. Instrum. Methods **A338**, 185 (1994).
3. CDF Collaboration, F. Abe *et al*, Phys. Rev. Lett., **70**, 713 (1993).
4. OPAL Collaboration, P.D. Acton *et al.*, Z. Phys. C **58** 387 (1993); OPAL Collaboration, P.D. Acton *et al.*, Z. Phys. C **63** 197 (1994).
5. For more details on all aspects of this analysis, see B. Abbott, Ph.D. Thesis, Purdue University (1994), unpublished.
6. H. Weerts, in proceedings of *9th Topical Workshop on Proton-Antiproton Collider Physics*, edited by K. Kondo and S. Kim, (Universal Academy Press, Tokyo, Japan, 1994).
7. J. Huth *et al.*, in proceedings of *Research Directions for the Decade, Snowmass 1990*, edited by E.L. Berger, (World Scientific, Singapore, 1992).
8. G. Marchesini and B.R. Webber, Nucl. Phys. **B310**, 461 (1988), version 5.8.
9. F. Carminati *et al.*, "GEANT Users Guide", CERN Program Library, 1991 (unpublished), version 3.14.

10. F. Paige and S. Protopopescu, Report No. BNL38034, 1986 (unpublished), versions 7.0 and 7.06 in the central and forward regions, respectively.
11. T. Sjostrand, Computer Phys. Comm. **39** (1986) 347; H.U. Bengtsson, T. Sjostrand, Comput. Phys. Comm. **46** (1987) 43, version 5.6.
12. W.T. Giele, E.W.N. Glover and D.A. Kosower, Nucl. Phys. **B**403, 633 (1993).
13. CTEQ Collaboration, J. Botts, *et al.*, Phys. Lett. **B304**, 159 (1993).
14. A.D. Martin, W.J. Stirling, R.G. Roberts, Phys. Lett. **B306**, 145 (1993): Erratum-*ibid* **B309**, 492 (1993).
15. S.D. Ellis and D.E. Soper, private communication; S.D. Ellis, Z. Kunszt, and D.E. Soper, Phys. Rev. Lett. **69** (1992) 3615.
16. P.N. Harriman, A.D. Martin, R.G. Roberts and W.J. Stirling, Phys. Rev. D **42** (1990) 798 and Phys. Lett. **B243** (1990) 421.